Intermolecular Self-Interactions of the Titanium Tetrahalides TiX_4 (X = F, Cl, Br)

Simon P. Webb and Mark S. Gordon*

Contribution from the Department of Chemistry, Iowa State University, Ames, Iowa 50011

Received September 18, 1998. Revised Manuscript Received December 21, 1998

Abstract: Ab initio calculations have been performed on the closed-shell molecules TiX_4 and Ti_2X_8 (X = F, Cl, Br) in order to determine the magnitude and the nature of the intermolecular self-interactions of the titanium tetrahalides. Geometry optimizations have been carried out using an effective core potential basis set with polarization, including the effects of dynamic electron correlation through second-order perturbation theory (MP2). The importance of higher order correlation effects is examined through coupled cluster single-point energy calculations. Basis set effects are investigated using MP2 single-point energy calculations with large all-electron basis sets. Ti_2F_8 is predicted to be a bound C_{2h} dimer with bridging bonds, lower in energy than the separated monomers by 10.5 kcal/mol. Ti_2Cl_8 and Ti_2Br_8 are predicted to be weakly bound dimers whose structures are that of associated monomers with overall D_{3d} point group symmetry. Ti_2Cl_8 is lower in energy than separated monomers by 4.9 kcal/mol. Transition states have been found that represent paths to halide exchange between monomers supporting experimental evidence for rapid halide exchange in liquid $TiCl_4$ and in mixed systems such as $TiCl_4/TiBr_4$.

Introduction

The titanium tetrahalides are considered to be among the most important titanium compounds as they are used as starting materials for the preparation of many organo-titanium systems.[1] This is especially true of $TiCl_4$, which is the precursor for a number of Ziegler−Natta catalysts.[1,2b,3] Due to the importance of this class of compounds, an understanding of their basic fundamental chemistry through experiment and *ab initio* calculations is an appropriate goal which has received considerable attention.

Gas-phase TiF_4 has been made by the reaction between $TiCl_4$ and NaF, and its infrared spectrum has been measured.[4] Confusion over peak assignments due to the possible range of products (TiF_nCl_{4-n}, $n = 0-4$) was eliminated by *ab initio* calculation of the vibrational frequencies of all these candidates, leading to the conclusion that only TiF_4 and $TiFCl_3$ were present.[5] Other theoretical studies have investigated the complexes between H_2CO and $TiCl_4$.[6] RHF geometry optimizations followed by MP2 single-point energies using a double-ξ quality basis set found that, within the $(H_2CO-TiCl_4)_2$ dimer, H_2CO was found to interact with $TiCl_4$ more strongly than in the monomer, illustrating the modification of the reactivity of the titanium tetrahalides due to their intermolecular interactions. Storey carried out several kinetic studies on the polymerization of isobutylene initiated by a dicumyl chloride/$TiCl_4$/pyridine system.[7] To explain an observed second-order kinetic dependence on $TiCl_4$ concentration, he considered two mechanisms: one of these involves the anion $Ti_2Cl_9^-$; the other involves the neutral dimer Ti_2Cl_8. Storey concluded that the former is the species involved. While the existence of $Ti_2Cl_9^-$ has been clearly demonstrated,[8] the existence of Ti_2Cl_8 has not. Storey's consideration of the neutral dimer is probably due to inconclusive reports in the literature of its existence. We now briefly consider experimental evidence of intermolecular self-interactions of the titanium tetrahalides.

Experiments have shown TiF_4 to be molecular with a coordination number of four in the gas phase and a polymer chain with a Ti coordination number of six in the solid state[9] (the exact structure is unknown). In contrast, gas phase *and* solid-state $TiCl_4$ and $TiBr_4$ are generally thought to be molecular with Ti coordination numbers of four.[9a] These observations are indicative of considerable attractive intermolecular interactions in the tetrafluoride and little or no attraction in the other tetrahalides. The lack of monotonic behavior of the melting and boiling points of the titanium tetrahalides[10] (see Table 1) provides further evidence of this. However, consideration of additional experimental evidence suggests there *may be* attractive intermolecular interaction in $TiCl_4$.

NMR studies done in 1967 by Pratt suggest that liquid $TiCl_4$ exhibits some "local order" which involves chlorine exchange between monomers.[11] Pratt based his conclusions on measurements made on both mixed $TiCl_4/VCl_4$ solutions and pure liquid

(1) Wailes, P. C.; Coutts, R. S. P.; Weigold, H. In *Organometallic Chemistry of Titanium, Zirconium, and Hafnium*; Academic Press: New york, 1974; Chapters 1−3.

(2) (a) Greenwood, N. N.; Earnshaw, A. In *Chemistry of the Elements*; Pergamon Press: New York, 1984. (b) *Ibid.* Chapter 21, p 1134. (c) Chapter 6, *Ibid.* p 222.

(3) (a) Sakai, S. *J. Phys. Chem.* **1994**, *98*, 12053. (b) Sobota P.; Utko, J.; Lis, T. *J. Organomet. Chem.* **1990**, 393, 349.

(4) (a) Beattie, I. R.; Jones, P. J. *J. Chem. Phys.* **1989**, *90*, 5209. (b) DeVore, T. C.; Gallaher, T. N. *J. Chem. Phys.* **1985**, *82*, 2512.

(5) Bauschlicher, C. W., Jr.; Taylor, P.; Komornicki, A. *J. Chem. Phys.* **1990**, *92*, 3982.

(6) (a) Branchadell, V.; Oliva, A. *J. Am. Chem. Soc.* **1992**, *114*, 4357. (b) Branchadell, V.; Oliva, A. *Inorg. Chem.* **1995**, *34*, 3433.

(7) (a) Storey, R. F.; Choate Jr., K. R. *Macromolecules* **1997**, *30*, 4799. (b) Storey, R. F.; Chisholm, B. J.; Brister, L. B. *Macromolecules* **1995**, *28*, 4055.

(8) Kistenmacher, T. J.; Stucky, G. D. *Inorg. Chem.* **1971**, *10*, 12.

(9) (a) Mousty-Desbuquoit, C.; Riga, J.; Verbist, J. J. *Inorg. Chem.* **1987**, *26*, 1212. (b) Euler, R. D.; Westrum, E. F. *J. Phys. Chem.* **1961**, *65*, 132.

(10) Clark, R. J. H. In *The Chemistry of Titanium and Vanadium*; Elsevier: Amsterdam, 1968; p 25.

(11) Pratt, D. W. Thesis, University of California, Berkeley, 1967.

10.1021/ja983339i CCC: $18.00
Published on Web 03/04/1999

Table 1. Melting and Boiling Points of the Titanium Tetrahalides[a]

	melting point/°C	boiling point/°C
TiF_4		284.0
$TiCl_4$	−24.0	136.4
$TiBr_4$	39.0	233.0
TiI_4	150.0	377.0

[a] Reference 10.

$TiCl_4$. The $TiCl_4/VCl_4$ mixture produced only *one* ^{35}Cl NMR signal, and the chemical shift of this signal was dependent on the $TiCl_4/VCl_4$ ratio. This led to the conclusion that there must be rapid exchange of chlorines in $TiCl_4/VCl_4$, possibly through dimers. Furthermore, the line width was greater than expected, which Pratt explained as "arising from an exchange not quite rapid enough to produce a complete collapse of the two signals". In pure $TiCl_4$, the ^{35}Cl NMR line width was found to be larger than expected and temperature dependent, becoming narrower on heating over a small temperature range (23−67 °C). Again it was concluded that there is rapid exchange of chlorines between monomers. The increased line width was thought to be due to superimposed lines resulting from different chlorine environments, based on the $TiCl_4/VCl_4$ result, possibly those in monomer and dimer species.

A study by Griffiths in 1968, using laser Raman spectroscopy, discovered an anomalous intensity distribution of the isotope fine structure in the spectrum of the totally symmetric mode of pure liquid $TiCl_4$.[12] Griffiths also observed a splitting of the asymmetric stretch band which disappeared on dilution of the pure $TiCl_4$ with CCl_4. He suggested dimer structures with bridging chlorines to explain his results. However, in 1971 Clark and Willis, who found the same anomalous intensity distribution, dismissed the suggestion of dimers and instead explained the result in terms of underlying hot bands.[13] In addition, Clark and Willis studied halogen exchange between $TiCl_4$ and $TiBr_4$ finding a random distribution of the five possible species. Rapid halide exchange in such a system was confirmed by an NMR study[14] which observed a single resonance peak for the mixture. In a 1974 study, Griffith, while abandoning the dimer structures he proposed earlier, insisted that the anomalous intensity distribution was due mainly to strong intermolecular interactions. Finally, an infrared spectroscopy study in 1985 claims to have discovered the presence of $TiCl_4$ dimers in argon matrixes at cryogenic temperatures, proposing structures similar to those suggested Griffiths in 1968.[16]

Obviously such contradictory conclusions mean that the question of the strength of intermolecular self-interactions in TiX_4 (X = F, Cl, Br) and the possible formation of dimers is unresolved. Moreover, there is agreement regarding the existence of halide exchange between monomers, but the mechanism of the exchange has not been established. *Ab initio* calculations would appear to be ideally suited to clarifying the situation.

Ab initio studies of the dimerization energies of other halide systems such as magnesium dihalide clusters,[17] zinc, cadmium, and mercury dihalide dimers,[18] and chlorogallane dimers[19] have proved useful in establishing and explaining trends in their intermolecular interactions and general reactivity. A study of titanium tetrahydride TiH_4 revealed a large attractive intermolecular interaction resulting in the formation of strongly bound Ti_2H_8 dimers with hydrogen bridges.[14] This may be explained by the electron deficiency of titanium and its desire for large coordination numbers due to its unfilled d shell. The introduction of lone pairs in the titanium tetrahalides results in species more complicated than the tetrahydride. Reliable determination of the magnitude and nature of the intermolecular self-interactions exhibited by the titanium tetrahalides and explanation of their differences is clearly desirable. In this paper, we will present results of an *ab initio* study in which we calculate dimerization energies of TiX_4, with X = F, Cl, and Br.

Presumably, the magnitude of any attractive or repulsive interactions between titanium tetrahalide monomers is dependent in part on effects due to the nature of the titanium−halide bond. This could include effects due to bond polarity and to titanium's electron deficiency. Steric effects may also play a role in the observed trends due to the increase in size of the halides down the group. We use the results of our study on the dimerization of titanium tetrahydride[20] as a reference and monitor directly the effect of halide replacement on monomer interaction.

Our aim is threefold: (1) to provide reliable quantitative information on the intermolecular self-interactions of TiX_4 (X = F, Cl, Br), (2) to assess the effect of substituents of varying size and electronegativity on intermolecular interaction and the dimerization process, and (3) to explore the potential energy surface by which halide exchange can occur between two monomers via dimers.

We use various methods, including population analysis, orbital localization, and energy decomposition to analyze *ab initio* wave functions in order to investigate these systems.

Computational Methods

Initially, geometry optimizations of the titanium tetrahalides TiX_4 (X = F, Cl, Br) and their dimers Ti_2X_8 were carried out at the RHF level of theory using the Stevens−Basch−Krauss−Jasien−Cundari effective core potential[21] (SBK) basis set with d polarization functions (F $\alpha = 0.800$, Cl $\alpha = 0.750$, Br $\alpha = 0.389$) added to halide atoms. This double-ζ quality basis set will be referred to as SBKP. For transition metals, SBK does not include the $3s^23p^6$ electrons as part of the effective core. The explicit treatment of these semicore electrons using a one-electron basis set has been found to be required for an adequate description of the electronic structure of transition metal atoms. Geometry optimizations were then done with the SBKP basis set using second-order perturbation theory (MP2)[22] to account for dynamic electron correlation.

All stationary points were characterized by calculating and diagonalizing the matrix of the second derivative of the energy (Hessian): no imaginary frequencies indicates a minimum on the potential energy surface; one imaginary frequency indicates a transition state.

Single-point energies using the coupled cluster method, CCSD(T),[23] with the SBKP basis set were carried out on selected structures to assess the effects of higher order dynamic electron correlation. In addition, for the fluorine and chlorine systems single-point MP2 energy calculations were carried out with all-electron basis sets to asses the adequacy of the SBK basis set. For titanium a triple-ζ (14s11p6d/10s8p3d) basis

(12) Griffiths, J. E. *J. Phys. Chem.* **1968**, *49*, 642.
(13) Clark, J. H.; Willis, C. J. *Inorg. Chem.* **1971**, *10*, 1118.
(14) Kidd, R. G.; Matthews, R. W.; Spinney, H. G. *J. Am. Chem. Soc.* **1972**, *94*, 6686.
(15) Griffiths, J. E. *Spectrochim. Acta* **1974**, *30A*, 169.
(16) Rytter, E.; Kvisle, S. *Inorg. Chem.* **1985**, *24*, 639.
(17) Axten, J.; Mendel, T.; Bock, C. W. *J. Phys. Chem.* **1994**, *98*, 7823.
(18) (a) Kaupp, M.; von Schnering, H. G. *Inorg. Chem.* **1994**, *33*, 4718. (b) Kaupp, M.; von Schnering, H. G. *Inorg. Chem.* **1994**, *33*, 2555.
(19) Duke, B. J.; Hamilton, T. P.; Schaefer, H. F., III *Inorg. Chem.* **1991**, *30*, 4225.
(20) Webb, S. P.; Gordon, M. S. *J. Am. Chem. Soc.* **1995**, *117*, 7197.
(21) (a) Cundari, T. R.; Stevens, W. J. *J. Chem. Phys.* **1993**, *98*, 5555. (b) Stevens, W. J.; Basch, H.; Krauss, M.; Jaisen, P. *Can. J. Chem.* **1992**, *70*, 612. (c) Stevens, W. J.; Basch, H.; Krauss *J. Chem. Phys.* **1984**, *81*, 6026.
(22) (a) Binkley, J. S.; Pople, J. A. *Int. J. Quantum Chem.* **1975**, *9*, 229. (b) Krishnan, R.; Pople, J. A. *Int. J. Quantum Chem.* **1978**, *14*, 91. (c) Frisch, M. J.; Head-Gordon, M.; Pople, J. A. *Chem. Phys. Lett.* **1990**, *166*, 275.
(23) Pople, J. A.; Head-Gordon M.; and Raghavachari, K. *J. Chem. Phys.* **1987**, *87*, 5968.

Table 2. Calculated and Experimental Ti−X Bond Lengths for the Tetrahedral TiX_4 Molecules (X = F, Cl, Br)

	bond lengths/Å		
	RHF/SBKP	MP2/SBKP	Experiment[a]
TiF_4	1.746	1.765	1.754
$TiCl_4$	2.183	2.171	2.170
$TiBr_4$	2.337	2.328	2.339

[a] Reference 33.

set was used. This consists of Wachter's basis set[24] with two additional sets of p functions[25] and a set of diffuse d functions.[26] For fluorine, we employed the triple-ζ (10s6p/5s3p) basis set of Dunning;[27] for chlorine, the triple-ζ (14s9p/8s4p) basis set of McLean and Chandler[28] was used. Polarization functions were added to this triple-ζ basis: f functions on the titanium ($\alpha = 0.40$),[20] two sets of d polarization functions on the halides, and diffuse s and p functions on the halides also. The 2d polarization function exponents and the diffuse sp function exponents are the default values in GAMESS.[29] This basis set is referred to as TZVP. To test for the level of convergence of this TZVP all-electron basis set, selected single-point MP2 energies were carried out retaining the above halide basis sets but with an expanded titanium basis set, denoted TZVP(g). This consists of the titanium triple-ζ basis described above plus one set of f ($\alpha = 0.591$) and g ($\alpha = 0.390$) functions and a set of diffuse s ($\alpha = 0.035$), p ($\alpha = 0.239$), and d ($\alpha = 0.0207$) functions. Exponents used here are optimized for correlated titanium atoms and are due to Glezakou and Gordon.[30] The semicore electrons, as well as the valence electrons in Ti ($3s^23p^64s^23d^2$), were correlated in all post Hartree−Fock calculations. Single-point energies determined at one level of theory (A) using geometries obtained at another level of theory (B) are denoted A//B.

The RHF and MP2 calculations were carried out using the electronic structure code GAMESS;[29] the largest MP2 single-point energy calculations (Ti_2Cl_8 with the TZVP(g) basis set), which involved 470 basis functions, required use of the newly implemented parallel algorithm of Fletcher et al.[31] The CCSD(T) single-point energies were done using Gaussian 92.[32]

Results and Discussion

TiX_4. The titanium tetrahalides TiX_4 (X = F, Cl, Br) were found to be tetrahedral at both the RHF and MP2 levels of theory. This is consistent with previous *ab initio* calculations[33] and gas-phase experiments.[34] Calculated and experimentally determined bond lengths and total energies are given in Tables 2 and 3, respectively.

Table 3. Total Energies (in Hartrees) of TiX_4 (X = F, Cl, Br) Calculated Using the SBKP basis set. Calculated using the all electron basis sets TZVP and TZVP(g)

(a) Calculated Using the SBKP Basis Set

	SBKP		
	RHF[a]	MP2[a]	CCSD(T)[b]
TiF_4	−153.19990	−154.20671	−154.23138
$TiCl_4$	−116.45762	−117.33226	−117.39495
$TiBr_4$	−110.29105	−111.14418	−111.18487

(b) Calculated Using the All-Electron Basis Sets

	MP2	
	TZVP[a]	TZVP(g)[a]
TiF_4	−1247.93521	−1247.96689
$TiCl_4$	−2687.76258	−2687.79513

[a] Geometry optimized at this level of theory. [b] Single-point energy calculated at the MP2/SBKP geometry. [c] Single-point energy calculated at the MP2/SBKP geometry.

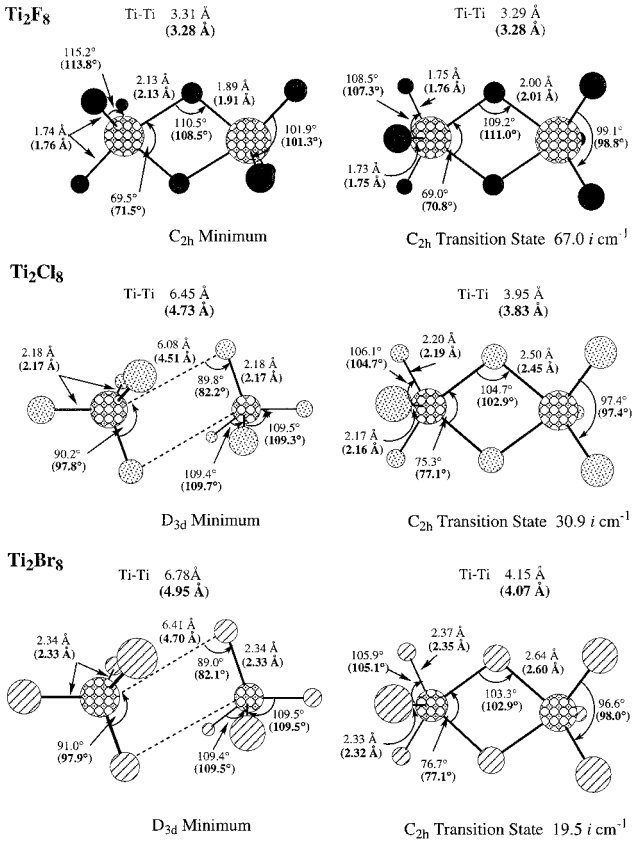

Figure 1. RHF and MP2/SBKP optimized structures for minima and transition states on the potential energy surface of Ti_2X_8 (X = F, Cl, Br). MP2 geometries are given in parentheses.

Ti_2X_8. The Ti_2X_8 dimers, which were found to be minima and transition states at the MP2/SBKP level of theory, are shown in Figure 1. The fluoride dimer minimum and all dimer transition states possess C_{2h} symmetry; the chloride and bromide minima possess D_{3d} symmetry. Energies of the dimers relative to the monomers can be seen in Table 4.

(a) Molecular Structure and Energetics. First we consider the molecular structures of the titanium tetrahalides and their dimers. Calculated Ti−X bond lengths in TiX_4 at the MP2/SBK level are in excellent agreement with available experimental data (see Table 2). It appears that for the TiX_4 monomers introduction of dynamic electron correlation has only a minimal effect on the calculated bond lengths. For TiF_4, the Ti−F bond

(24) Wachters, A. J. H. *J. Chem. Phys.* **1970**, *55*, 716.
(25) Hood, D. M.; Pitzer, R. M.; Schaefer, H. F. *J. Chem. Phys.* **1979**, *71*, 705.
(26) Rappe, A. K.; Smedley, T. A.; Goddard, W. A. *J. Phys. Chem.* **1981**, *85*, 2607.
(27) Dunning, T. H. *J. Chem. Phys.* **1971**, *72*, 5639.
(28) McLean, A. D.; Chandler, G. S. *J. Chem. Phys.* **1980**, *72*, 5639.
(29) Schmidt, M. W.; Baldridge, K. K.; Boatz, J. A.; Jensen, J. H.; koseki, S.; Matsunaga, N.; Gordon, M. S.; Ngugen, K. A.; Su, S.; Windus, T. L.; Elbert, S. T.; Montgomery, J.; Dupuis, M. *J. Comput. Chem.* **1993**, *14*, 1347.
(30) Glezakou, V.-A.; Gordon, M. S. *J. Phys. Chem.* **1997**, *101*, 8714.
(31) (a) Fletcher, G. D.; Schmidt, M. W.; Gordon, M. S. *Adv. Chem. Phys.*, in press. (b) Fletcher, G. D.; Rendell, A. P.; Sherwood, P. *Mol. Phys.* **1997**, *91*, 431.
(32) Frisch, M. J.; Trucks, G. W.; Head-Gordon, M.; Gill, P. M. W.; Wong, M. W.; Foresman, J. B.; Johnson, B. G.; Schlegel, H. B.; Robb, M. A.; Replogle, E. S.; Gomperts, R.; Andres, J. L.; Raghavachari, K.; Binkley, J. S.; Gonzalez, C.; Martin, R. L.; Fox, D. J.; DeFrees, D. J.; Baker, J.; Stewert, J. J. P.; Pople, J. A.; GAUSSIAN92; GAUSSIAN, INC.: Pittsburgh, PA, 1992.
(33) (a) Russo, T. V.; Martin, R. L.; Hay, P. J. *J. Chem. Phys.* **1995**, *102*, 8023. (b) Russo, T. V.; Martin, R. L.; Hay, P. J.; Rappé, A. K. *J. Chem. Phys.* **1995**, *102*, 9315.
(34) (a) Moore, E. A.; Healy, A. *J. Chem. Soc., Faraday Trans.* **1995**, *91*, 1735. (b) Dobbs, K. D.; Hehre, W. J. *J. Comput. Chem.* **1987**, *8*, 880. (c) Morito, Y.; Vehara, H. *J. Chem. Phys.* **1966**, *45*, 4543.

Table 4. (a, top) Calculated Energies (kcal/mol) of Ti_2X_8 Relative to TiX_4 (X = F, Cl, Br) and MP2 Zero-Point Energy Corrections Using the SBKP Basis Set and (b, bottom) Calculated MP2 Single-Point Energies (kcal/mol) of Ti_2X_8 Relative to TiX_4 (X = F, Cl, Br) with the All-Electron Basis Sets TZVP andTZVP(g)

	SBKP			
	RHF[a]	MP2[a]	ZPE[b]	CCSD(T)[c]
Ti_2F_8 min	−8.6	−14.3	+1.1	−16.8
Ti_2F_8 TS	−6.1	−12.4	+1.0	
Ti_2Cl_8 min	−0.3	−5.2	+0.3	−4.6
Ti_2Cl_8 TS	+23.5	+5.2	+0.6	
Ti_2Br_8 min	−0.1	−6.3	+0.2	
Ti_2Br_8 TS	+26.0	+6.6	+0.3	

	MP2	
	TZVP[c]	TZVP(g)[c]
Ti_2F_8 min	−9.6	−10.5
Ti_2F_8 TS	−7.6	−8.7
Ti_2Cl_8 min	−4.5	−4.9
Ti_2Cl_8 TS	+5.0	+4.1

[a] Geometry optimized at this level of theory. [b] Calculated at the MP2/SBKP level of theory.[c] Single point energy calculated at the MP2/SBKP geometry.

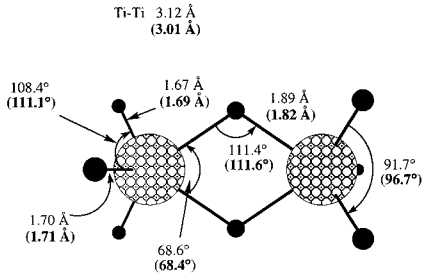

Energies of C_{2h} Ti_2H_8 relative to $2TiH_4$ in kcal/mol.

RHF/SBKP(opt)	MP2/SBKP(opt)
- 23.7	- 40.1

Figure 2. Calculated energies (kcal/mol) of C_{2h} Ti_2H_8 relative to $2TiH_4$ (opt) indicates that the geometry has been optimized at that level of theory. RHF bond lengths and angles are in normal typeface; MP2 bond lengths and angles are in bold typeface.

length is increased by only ∼0.02 Å; for $TiCl_4$ and $TiBr_4$, the Ti−X bond lengths are both shortened by only ∼0.01 Å.

The Ti_2X_8 structures found (see Figure 1) indicate large substituent effects due to the halide ligands. Only double halide bridged $(\mu\text{-X})_2$ Ti_2X_8 dimers were found, whereas Ti_2H_8 isomers[20] with a $(\mu\text{-H})_3$ bridging arrangement have been shown to be more stable than those with a $(\mu\text{-H})_2$ bridging arrangement. Other structural effects can be seen by comparing a $(\mu\text{-H})_2$ Ti_2H_8 minimum energy structure (see Figure 2) with the tetrahalide dimer structures. The analogous dibridged halide structures are actually transition states for exchanging the bridging atoms (see Figures 1 and 3). As expected, the halide bond lengths are longer than in the hydride (MP2/SBKP optimized geometries). This increase is modest for the fluoride, with the Ti−Ti separation increasing by ∼0.3 Å, the bridging bond lengths increasing by ∼ 0.2 Å, and the terminal bond lengths increasing by 0.07 Å or less. This is indicative of the small size and large electronegativity of fluorine, which results in short bonds. There is a more substantial increase in these same parameters on going from the fluoride to the chloride (∼0.5, ∼0.4, and ∼0.4 Å), followed by a modest increase on going from chloride to bromide (∼0.25, ∼0.15, and ∼0.15 Å). The large differences between the fluoride and chloride are clearly a result of both the increased size and lower electronegativity of Cl. The electronegativities of Cl and Br are very similar; the changes on going from chloride to bromide, then, are due primarily to the larger size of Br. Dynamic electron correlation effects on the transition-state halide dimer *geometries* are found to be minimal (see Figure 1).

In the halide dimer minima, the substituent effect is even more apparent. The fluoride dimer retains its bridging bonds, though now the bridge is no longer symmetric with Ti−F−Ti bridging bond lengths of 1.91 and 2.13 Å (MP2/SBKP optimized geometries). This effect is exaggerated greatly in the chloride and bromide where covalent bridging bonds no longer exist. Instead, these structures resemble weakly bound van der Waals complexes. In fact, within the dimers the geometries of the TiX_4 moieties are hardly distorted from those of the separated monomers, with little change from a purely tetrahedral arrangement (see Table 2 and Figure 1). For the fluoride minimum, dynamic electron correlation has only a minor effect on the structure; however, for the chloride and bromide, the effect is large. Dynamic electron correlation allows the tetrahalide moieties in these dimers to approach much more closely. The Ti−Ti separation is reduced by 1.72 and 1.83 Å in the chloride and bromide, respectively, on going from RHF to MP2 optimized structures.

We now consider energetics (see Table 4) discussing, unless otherwise stated, the classical potential energy surface (no zero-point energy (ZPE) correction) at 0 K (see following section for ZPE and temperature effects). Comparison with the Ti_2H_8 dimer reveals that the introduction of halides makes the dimerization process much less favorable. At the RHF/SBKP level of theory, the fluoride dimer minimum and transition state are lower in energy than the separated monomers by 8.6 and 6.1 kcal/mol, respectively. For the chloride and bromide, the transition states are higher in energy than the separated monomers by 23.5 and 26.0 kcal/mol, respectively. The value for the chloride is in good agreement with that of Branchadell and Oliva,[6b] who predicted 20.7 kcal/mol at a similar level of theory. The chloride and bromide minima are essentially isoenergetic with their separated monomers (dimerization energies of − 0.3 and − 0.1 kcal/mol, respectively). This is consistent with the notion that these are weakly bound van der Waals species, since dispersion effects are not accounted for at the Hartree−Fock level of theory.

Table 4 shows that inclusion of dynamic electron correlation through MP2 using the SBKP basis set lowers the energies of all the dimers with respect to the monomers. The fluoride dimer minimum and transition state are now predicted to be lower in energy than two separated monomers by 14.3 and 12.4 kcal/mol, a difference of −5.7 and −6.3 kcal/mol, respectively. The chloride and bromide minimums are predicted to be weakly bound dimers with dimerization energies of −5.2 and −6.3 kcal/mol, respectively. However, the correlation effect is clearly largest for the chloride and bromide transition states whose energies are lowered by 18.3 and 19.4 kcal/mol, respectively, at the MP2/SBKP level, relative to RHF/SBKP. This suggests that electron−electron repulsion is large in these bound dimer conformations and therefore steric effects are playing a role in their unfavorable energetics.

To assess the effect of including dynamic electron correlation in the geometry optimizations on the energetics, single-point MP2/SBKP energies were calculated at RHF/SBKP optimized geometries. For both fluoride dimers and for the chloride and bromide transition states, MP2//RHF reproduce the MP2//MP2 energies very well, giving values of −14.1, −12.2, +6.2, and +7.3 kcal/mol. For the chloride and bromide minima, where

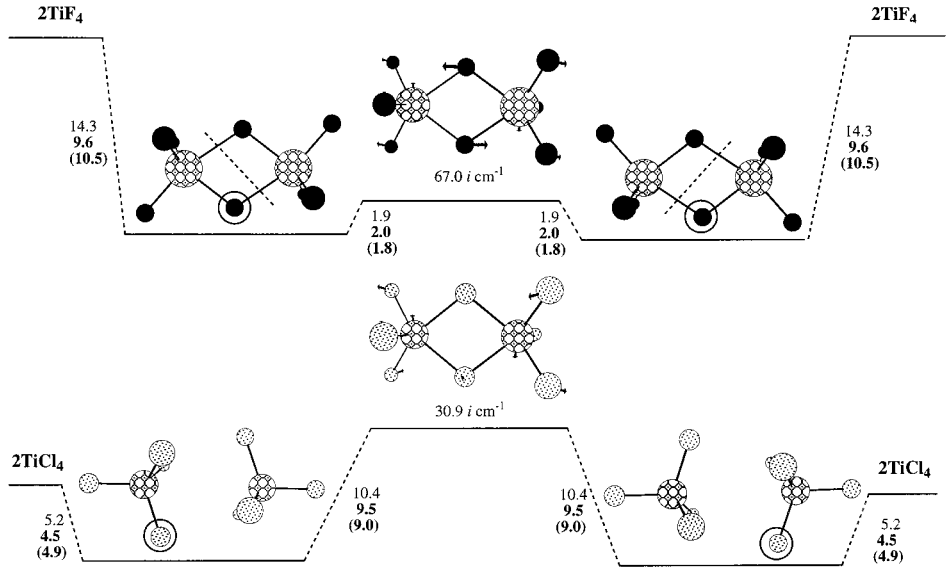

Figure 3. Possible mechanisms for halide exchange in $2TiF_4$ and $2TiCl_4$. Energies are in kilocalories per mole. MP2/SBKP energies (optimized structures) are in normal typeface, MP2/TZVP single-point energies are in bold face, and MP2/TZVP(g) single-point energies are boldface and in parentheses. Circles indicate halides that are exchanged.

Table 5. Free Energies, ΔG, of Dimerization of TiF_4 and $TiCl_4$ (kcal/mol) Calculated at the MP2/SBKP Level of Theory

	ΔG of dimerization									
	−273.15 °C	−261.15 °C	−196.0 °C	−60.0 °C	−23.0 °C	25.0 °C	67.0 °C	138.0 °C	285.0 °C	320.0 °C
					Vibrational Effects Only					
Ti_2F_8 min	−13.2	−13.2	−13.5	−15.2	−15.8	−16.7	−17.6	−19.2	−23.0	−24.0
Ti_2F_8 TS	−11.4	−11.4	−11.8	−13.5	−14.1	−14.9	−15.7	−17.2	−20.6	−21.5
					Rotational + Translational + Vibrational Effects Included					
Ti_2F_8 min	−13.2	−12.4	−10.9	−6.4	−5.2	−3.6	−2.3	−0.1	4.3	5.3
Ti_2F_8 TS	−11.4	−11.2	−9.2	−4.7	−3.4	−1.8	−0.4	1.9	6.7	7.9
					Vibrational Effects Only					
Ti_2Cl_8 min	−4.9	−4.9	−5.7	−9.1	−10.2	−11.9	−13.3	−16.0	−21.9	−23.3
Ti_2Cl_8 TS	5.8	5.8	5.3	3.4	2.7	1.8	0.9	−0.8	−4.6	−5.6
					Rotational + Translational + Vibrational Effects Included					
Ti_2Cl_8 min	−4.9	−5.6	−2.8	0.6	1.5	2.5	3.4	4.9	7.9	8.6
Ti_2Cl_8 TS	5.8	5.1	8.2	13.2	14.5	16.2	17.7	20.2	25.3	26.5

dynamic electron correlation has a large structural effect, this is not the case. MP2/SBKP single-point energies give dimerization energies of −1.8 and −1.5 kcal/mol for the chloride and bromide, respectively, compared with −5.2 and −6.3 kcal/mol for the MP2//MP2 energies. Inclusion of dynamic electron correlation in the geometry optimization, then, is essential to properly describe the weakly bound dimers.

Higher order correlation effects introduced through CCSD(T)//MP2 calculations with the SBKP basis set (see Table 4a) are smaller, but not trivial. The difference between the MP2 and CCSD(T) dimer energies relative to separated monomers is −2.5 and +0.6 kcal/mol for the Ti_2F_8 minimum and Ti_2Cl_8 minimum, respectively.

It is clear from MP2/TZVP and MP2/TZVP(g) energies at the MP2/SBKP optimized geometries that the SBKP basis set overestimates the exothermicity of the fluoride dimer but appears to do very well for the chloride (see Table 4). We expect that the SBKP basis set is also reliable for the bromide calculation. The largest basis set, TZVP(g), demonstrates convergence of dimerization energies to ∼ 1 kcal/mol or less.

(b) Melting and Boiling Point Trends, Temperature Effects, and Halide Exchange. TiF_4 has a higher boiling point than $TiCl_4$, even though it has a lower molecular mass (see Table 1). This suggests larger intermolecular interactions in TiF_4 than in $TiCl_4$. Other experimental evidence[9] indicates that TiF_4 forms polymeric chains in the solid phase, while $TiCl_4$ remains in discrete molecular units, again suggesting larger intermolecular interactions in TiF_4. The dimerization energies calculated on the classical surfaces at 0 K during this study (see Table 4b) show the dimerization energy of TiF_4 (−10.5 kcal/mol) to be more than twice that of $TiCl_4$ (−4.9 kcal/mol). So, according to these calculations, Ti_2F_8 is a bound dimer with bridging bonds, which is consistent with the formation of polymer chains, while the Ti_2Cl_8 minimum is a weakly bound van der Waals dimer, consistent with the tetrahedral structure seen even in the solid. $TiCl_4$ and $TiBr_4$ exhibit almost equal attractive intermolecular self-interactions consistent with the fact that their boiling/melting points resume the trend expected based only on molecular mass. According to this somewhat simplistic comparison, the calculated dimerization energies are entirely consistent with the structure and melting and boiling point trends of the titanium tetrahalides.

A more correct approach is to consider free energies of dimerization, ΔG, for a range of temperatures (see Table 5). ΔG values for the fluoride and chloride systems that include only vibrational effects are shown as well as values that include rotational, translational, and vibrational effects. To relate the properties of a dimer system to the melting and boiling points in the bulk, it is necessary to consider when it is appropriate to include or exclude rotational and translational effects in the

Table 6. Harmonic Vibrational Frequencies for T_d $TiCl_4$ and D_{3d} Ti_2Cl_8 Calculated at the MP2/SBKP Level of Theory

vibration	IR intens/km mol^{-1}	frequency/cm^{-1}	exptl frequency/cm^{-1}	IR/Raman activity
		$TiCl_4$ T_d		
ν_2 sym bend	0.0	123.5	121[a]	R
ν_4 asym bend	3.6	142.2	137[a]	IR,R
ν_1 sym str	0.0	396.2	389[a]	R
ν_3 asym str	226.4	521.1	524[b], 501[a]	IR,R
		Ti_2Cl_8 D_{3d}		
sym bend	0.0	122.1	123[c]	R
sym bend	0.0	143.7	142[c]	R
sym bend	0.0	144.6		R
sym str	0.0	397.3	389[c]	R
sym str	0.0	514.8	492[c]	R
sym str	0.0	522.2	510[c]	R
asym bend	0.0	127.2		IR
asym bend	12.9	136.9		IR
asym bend	6.1	142.1		IR
asym str	0.2	397.0	390[b]	IR
asym str	514.2	515.0	503[b]	IR
asym str	370.8	530.1	544[b]	IR

[a] Raman spectrum of 1:3 $TiCl_4/CCl_4$.[12] [b] IR spectrum, low-temperature matrix experiment.[16] [c] Raman spectrum of pure $TiCl_4$.[12]

calculation of ΔG. For the temperature range in which the bulk is solid, rotational and translational effects clearly should not be included; in the gas-phase temperature range, they clearly should. For liquid phase (applicable to $TiCl_4$), rotations and translations will be greatly hindered but will not be totally absent; however, it is more appropriate to disregard them than to include them. The appropriate ΔG values in Table 5, are consistent with the properties of bulk TiF_4 and $TiCl_4$. Below the boiling point of bulk TiF_4 (284.0 °C), dimerization of TiF_4 is thermodynamically favored by up to 19.2 kcal/mol; above its boiling point, the dimer minimum is less stable than separated monomers by 4.3 kcal/mol. This is consistent with polymeric chains in the solid phase and tetrahedral monomers in the gas phase. For solid-state and liquid-state temperatures of bulk $TiCl_4$, there is an attractive intermolecular interaction of up to 13.3 kcal/mol. Just above the boiling point of $TiCl_4$ (at 138.0 °C), separated monomers are thermodynamically more stable than the van der Waals dimer; that is, there is a repulsive interaction of 4.9 kcal/mol. This is consistent with local order involving attractive interactions in the liquid phase and monomers in the gas phase.

Pratt suggested that chlorine exchange between tetrachloride monomers may be a possible explanation for unexpected results in his NMR experiments.[11] Multiple products resulting from the mixing of $TiCl_4$ and $TiBr_4$ also suggests rapid halide exchange.[13,14] The transition states shown in Figure 1 represent possible paths to fluorine exchange within $2TiF_4$ and chlorine exchange within $2TiCl_4$ (also see Figure 3). First we briefly consider the classical potential energy surface at 0 K for these processes, as data from the full range of basis sets are available; subsequently, ΔG values will be considered.

For the fluoride, the entire exchange process is lower in energy than the separated monomers. There is a small barrier (1.9 kcal/mol) between the minima at the MP2/TZVP level; this creates a path to the exchange of bridging fluorines. It appears that while the SBKP basis set predicts the dimer well to be too low in energy compared to the TZVP(g) basis set, it predicts the barrier to fluorine exchange very well. The transition state leading to chlorine exchange is higher in energy than the separated monomers by 4.1 kcal/mol at the MP2/TZVP(g) level. This value represents the effective barrier that approaching monomers must overcome to achieve chlorine exchange. Monomers that come together and are trapped in the minima wells are only weakly bound by 4.9 kcal/mol. The SBKP basis set gives reliable energies for dimerization and exchange in the chloride system.

Now consider ΔG's at the MP2/SBKP level (see Table 5). At solid-state temperatures, it is only appropriate to consider exchange in the context of matrix-isolated dimers.[16] The qualitative and quantitative picture of exchange at these very low temperatures is hardly changed from that shown in Figure 3. For the fluoride system at 285.0 °C, Table 5 shows that the barrier to exchange is 6.7 kcal/mol, suggesting that exchange is still possible in the gas phase. For the liquid-phase temperature range of the chloride system (only vibrational effects considered), the barrier to exchange of chlorine between separated monomers is between 2.7 and 0.9 kcal/mol. The barrier, then, is lowered in the temperature range −23.0 to 67.0 °C by 1.8 kcal/mol. This trend is consistent with more rapid exchange at higher temperatures, as suggested by Pratt to explain temperature-dependent line widths. At 138.0 °C the barrier to exchange of chlorines is 20.2 kcal/mol, suggesting exchange is much less likely in the gas phase. We have not presented ΔG's for the bromide system, but on the basis of the energetics presented in Table 4 conclude that it will exhibit behavior similar to that in the chloride system.

(c) Calculated Harmonic Vibrational Frequencies. The calculated harmonic vibrational frequencies of the monomer and dimer structures facilitate a direct examination of the effects of monomer association on the $TiCl_4$ fundamentals (see Table 6). We have not carried out a detailed study of isotope effects on the Raman active modes and so cannot determine whether the anomalous intensity distribution of the isotope fine structure of ν_1 in pure liquid $TiCl_4$[12,13] is due to monomer association and the resulting perturbation of the vibrational force fields as has been suggested.[15,35] However, simply by examination of the Raman active modes in the monomer and dimer minima we can determine whether monomer association is responsible for the splitting of the ν_3 mode observed by Griffiths.[12] Similarly by examination of infrared active modes, we can comment on the IR frequencies observed in Rytter and Kvisle's low-temperature matrix experiment.[16]

The calculated frequencies for $TiCl_4$ are in good agreement with previous work.[5,33b] Experimental frequencies from the Raman spectrum of a 1:3 mixture of $TiCl_4/CCl_4$ are shown for comparison. These Raman frequencies are themselves in close

(35) Kroto, H. W.; Teixeira-Dias, J. J. C. *Mol. Phys.* **1970**, *18*, 773.

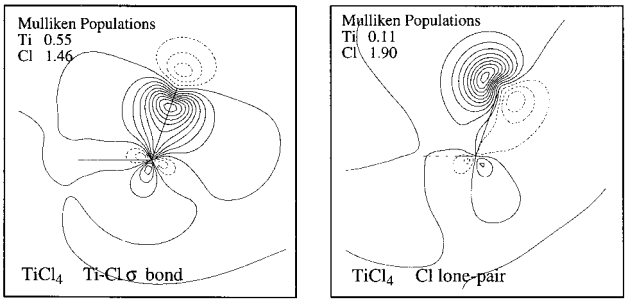

Figure 4. LMO plot of a Ti−Cl σ bond and Cl lone pair in $TiCl_4$. The contour increments are 0.05 bohr$^{3/2}$.

agreement with those measured in the gas phase by IR spectroscopy[36] (symmetric mode frequencies were derived from observed combination bands).

The calculated vibrational frequencies for D_{3d} Ti_2Cl_8 are either IR or Raman active. The Raman active modes, indicated by R in the far right-hand column of Table 6, may be compared to those found by Griffith for pure liquid $TiCl_4$. The calculated modes show that interactions in the weakly bound dimer could be responsible for the splitting of the ν_3 mode. The calculated frequency of the ν_3 mode of T_d $TiCl_4$ is 521.1 cm^{-1}. Table 6 shows that monomer association in D_{3d} Ti_2Cl_8 splits this mode into 514.8 and 522.2 cm^{-1}. However, the calculated splitting is smaller than the observed one (7.4 cm^{-1} compared to 18 cm^{-1}).

The IR active modes can be compared to those observed by Rytter and Kvisle.[16] Although comparison of calculated frequencies and those obtained in matrix isolation experiments is difficult at the low-frequency end due to interaction with the matrix,[20,37] based on Table 6 it is possible that the weakly bound dimer could be responsible for some of the extra peaks observed. The calculated frequency at 397.0 cm^{-1} corresponds to a stretching vibration that is symmetric for each monomer unit (like ν_1 in the separated monomer) within the weakly bound dimer, but as the stretching motion is in the opposite direction for each monomer unit it is asymmetric overall, thereby making the mode IR active. Its activity and therefore its intensity in the experiment may well be enhanced by interaction with the matrix, possibly resulting in the peak experimentally observed at 390 cm^{-1}. Other experimental peaks lie at 503, 544, and 524 cm^{-1}; the first two we assign to dimer asymmetric stretches, the last one to a monomer asymmetric stretch (assuming monomers are present as well as dimers). These assignments are different from those by Rytter and Kvisle. We cannot account for the observed frequency at 456 cm^{-1}.

(d) Bonding. The method of Edmiston and Ruedenberg[38] was used to localize the molecular orbitals in order to examine the nature of the bonding in the titanium halide systems. Plots of the localized molecular orbitals (LMOs) resulting from RHF/SBKP localization calculations at the MP2/SBKP geometries for the chloride monomer and transition-state dimer (C_{2h} Ti_2Cl_8 structure in Figure 1) are shown in Figures 4 and 5. Similar plots for the fluoride and bromide systems are available as Supporting Information.

Figure 4 shows a Ti−Cl σ bond LMO and a Cl lone-pair LMO which clearly reveals back-bonding to the Ti. Such back-bonding is also seen in the fluoride and bromide systems. Mulliken populations of localized orbitals are highly basis set dependent and inadequate for a truly meaningful assignment of electrons to Ti and X (X = F, Cl, Br). However, the method

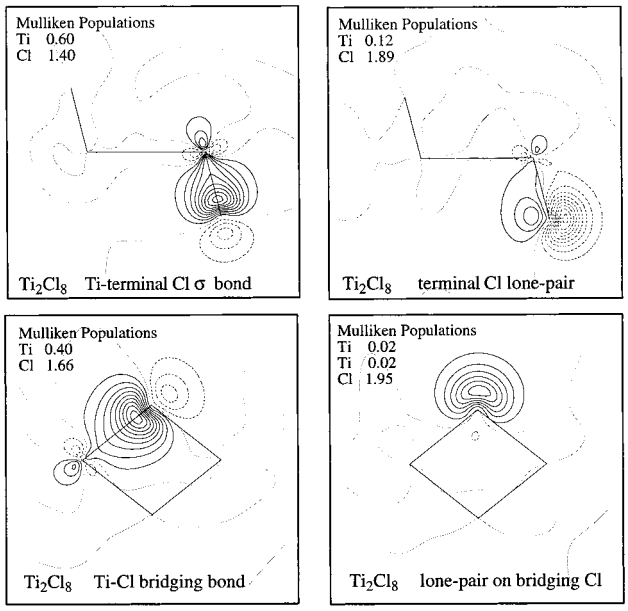

Figure 5. LMO plots of a Ti−Cl σ bond, Cl lone pairs, and a Ti−Cl bridging bond in the Ti_2Cl_8 transition state. The contour increments are 0.05 bohr$^{3/2}$.

is useful in determining trends in a series of molecules where an equivalent basis set is used throughout. Mulliken populations of the σ bonds confirm the expected trend in this series of molecules, revealing a highly polarized Ti−F bond and Ti−Cl and Ti−Br bonds that are still polarized but much less so. Populations of the lone-pair LMOs are indicative of the trend in the degree of back-bonding. Ti Mulliken populations in the TiF_4, $TiCl_4$, and $TiBr_4$ halide lone-pair LMOs are 0.06, 0.11, and 0.11, respectively. This suggests the degree of back-bonding follows the trend F < Cl = Br, though the differences are clearly very small.

Figure 5 shows selected LMOs of the C_{2h} Ti_2Cl_8 transition state. The LMO plots involving the terminal chlorine show a Ti−Cl σ bond and also the same kind of back-bonding character seen in the monomers (see Figure 4). Only one of four equivalent bridge LMOs is shown. The bridging arrangement is not a 3-center, 2-electron bond like that found in Ti_2H_8;[20] the LMOs clearly show participation of "lone-pair" electrons in the bridges resulting in a Ti−Cl−Ti bridge made up of two 2-center, 2-electron bonds. In total, the two chlorines in this arrangement donate 6 electrons and the titaniums donate 2 electrons to the bridges. Therefore, each of the bridging chlorines has two remaining nonbonding lone pairs (one is shown). The Ti_2F_8 and Ti_2Br_8 transition states as well as the Ti_2F_8 minimum have a bonding arrangement that looks similar to that in the Ti_2Cl_8 transition state. As the Ti_2Cl_8 and Ti_2Br_8 minima are weakly bound dimers with no bridging bonds, any perturbation of the monomer LMOs is not visually apparent.

(e) Dimerization Process. In a study on the dimerization of BF_3, Nxumalo and Ford[39] discounted several dimer structures that they predicted to be exothermically stable with respect to monomers. Their reason was an energy barrier that, they claimed, resulted from large unfavorable distortion energies of the monomers. In fact, their approach, which separates the energetics of the dimerization process into two distinct stages, (1) distortion of the monomers and (2) reaction of the distorted monomers to form a dimer, produces an artificial barrier. Such

(36) Hawkins, N. J.; Carpenter, D. R. *J. Chem. Phys.* **1955**, *23*, 1700.
(37) Webb, S. P.; Gordon, M. S. *J. Am. Chem. Soc.* **1998**, *120*, 3846.
(38) Edmiston, C.; Ruedenberg, K. *Rev. Mod. Phys.* **1963**, *35*, 457.
(39) Nxumalo, L. M.; Ford, T. A. *J. Mol. Struct. (THEOCHEM)* **1995**, *357*, 59.

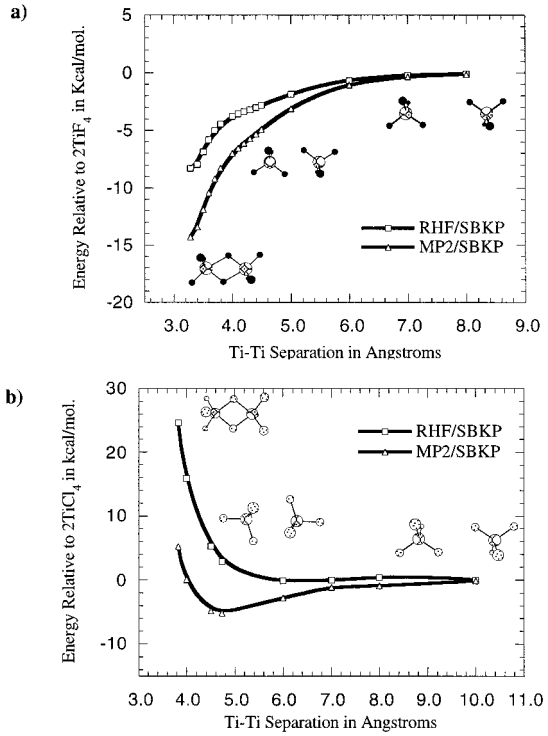

Figure 6. (a) Ti_2F_8 energy and (b) Ti_2Cl_8 energy (kcal/mol) relative to $2TiF_4$ and $TiCl_4$, respectively, versus Ti−Ti separation. The plots labeled MP2/SBKP are of energies from MP2/SBKP constrained optimizations; the plots labeled RHF/SBKP are of RHF/SBKP single-point energies at MP2/SBKP constrained geometries.

a barrier will *always* appear if the monomer geometries are significantly distorted in the dimer. In reality, the energetics of the process of dimerization are determined by a *continuous* competition between endothermic effects due to internal monomer structural distortion and exothermic effects due to monomer−monomer interaction, during the approach of the monomers as well as at the end point.

A more meaningful approach to determine whether a barrier exists is to carry out a number of constrained geometry optimizations for which only the distance between monomers is constrained (for example, constrain the Ti−Ti distance only), thereby creating a "reaction path" to dimerization. This method was used to establish that there is no energy barrier to the dimerization of TiH_4[20] and is applied here to TiF_4 and $TiCl_4$.

The constrained optimizations were carried out on the $2TiF_4$ and $2TiCl_4$ systems at the MP2/SBKP level; RHF/SBKP energies at these points are also plotted (see panels a and b of Figure 6, respectively). As point group symmetry was constrained to be C_{2h}, the paths shown are not necessarily the minimum energy paths; nonetheless, they establish that the dimerization of TiF_4 and $TiCl_4$ is a barrierless process (as opposed to the halide exchange processes, which are not barrierless (see Figure 3)).

Localized Charge Distribution (LCD) Analysis. To demonstrate the validity of our argument that the energetics of the process of dimerization are governed by a continuous competition between endothermic monomer distortion and exothermic monomer interaction, we have carried out an energy decomposition. The LCD analysis has proved to be a useful tool in understanding intermolecular interactions.[40] It decomposes the total energy of the system into potential and kinetic energies of

(40) (a) Jensen, J. H.; Gordon, M. S. *Acc. Chem. Res.* **1996**, *29*, 536. (b) Jensen, J. H.; Gordon, M. S. *J. Am. Chem. Soc.* **1995**, *99*, 8091. (c) England, W.; Gordon, M. S. *J. Am. Chem. Soc.* **1971**, *93*, 4649.

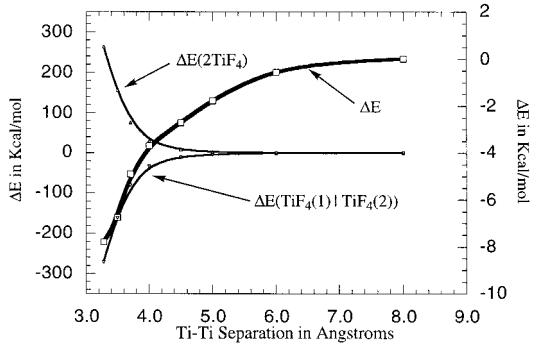

Figure 7. Change in total energy (boldface curve labeled ΔE, right y-axis), internal $\Delta E(2TiF_4)$, and interaction $\Delta E(TiF_4(1) \mid TiF_4(2))$ (left y-axis). Energies are relative to those at a Ti−Ti separation of 8 Å.

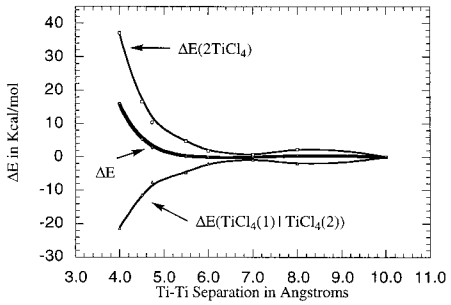

Figure 8. Change in total RHF energy (boldface curve labeled ΔE), internal $\Delta E(2TiCl_4)$, and interaction $\Delta E(TiCl_4(1) \mid TiCl_4(2))$. Energies are relative to those at a Ti−Ti separation of 10 Å.

LMOs and the interactions between them. We have carried out the analysis at the RHF level at points on the energy paths plotted in Figure 6.

The LCD analysis requires that a local nuclear charge distribution is assigned to each LMO. For semicore LMOs, Ti was assigned a nuclear charge of 2; for the Ti−X bond LMOs, Ti and X were each assigned a nuclear charge of 1; and for the X lone-pair LMOs, X was assigned a nuclear charge of 2. Note that these assignments were defined in the separated monomers and were applied consistently as the monomers approached each other. The LCD analysis allows us to determine the total internal energies of the monomers and the total interaction energy between them along the reaction path. This is done by summing the relevant individual LMO contributions.The resulting plots are shown in Figures 7 and 8.

In Figures 7 and 8, the bold curve is the total energy and is the sum of the remaining two curves, which are the total internal energy of the monomers ($\Delta E(2TiX_4)$) and the total interaction energy between the monomers ($\Delta E(TiX_4(1)|TiX_4(2))$). Clearly one can make a general observation that the internal energy goes up and the interaction energy goes down during these dimerization processes and the total energy along the path is the result of the competition between these two effects. In the fluoride system (Figure 7), the RHF dimerization process is barrierless and the resulting dimer is exothermic by 8 kcal/mol relative to separated monomers. In this case, the favorable monomer interaction dominates the unfavorable structural deformations. In the chloride system (Figure 8), the RHF total energy remains the same as that of the separated monomers (MP2 is required to observe the weakly bound minimum, see Figure 6b) until a Ti−Ti separation of less than 6 Å, and then the total energy relative to the monomers increases rapidly as the transition state Ti−Ti separation is approached. So, in this case, the interaction and structural deformation effects roughly cancel until a Ti−Ti separation of ∼6 Å and then the

endothermic structural deformation effects begin to dominate. This is suggestive of steric effects.

Conclusions

The titanium tetrahalides TiX_4 (X = F, Cl, Br) are all found to have attractive intermolecular interactions. TiF_4 possesses the largest attractive interaction, forming a bound dimer. Smaller interactions were found for $TiCl_4$ and $TiBr_4$; in these cases, only weakly interacting van der Waals dimers are predicted. This is consistent with known experimental data which suggest that solid-state TiF_4 is a bridged polymer chain, and solid-state $TiCl_4$ and $TiBr_4$ remain molecular in structure. The predicted interactions and ΔG's of dimerization are also consistent with the nonmonotonic behavior of the titanium tetrahalide melting points.

Transition states with symmetrically equivalent bridging halides were found. These represent possible routes to halide exchange between monomers.

Comparison of calculated and experimental vibrational frequencies of the chloride system suggests that splitting of the ν_3 mode in Raman studies could be due to interactions in the weakly bound van der Waals dimer. In addition, calculated frequencies which are IR active suggest some of the peaks seen in a low-temperature IR matrix experiment could be due to such dimers.

Dynamic correlation, introduced through MP2, was found to be very important for energetics for all the dimer structures studied. It was found to be less important for determining structures of the fluoride minimum and transition state and the chloride and bromide transition states. However, inclusion of dynamic correlation was found to be essential for geometry optimizations of the chloride and bromide minima. Higher order correlation effects introduced through CCSD(T) were found to have little effect.

The effective core potential basis set SBKP was found to overestimate the dimerization energy of TiF_4, with a dimerization energy of −14.3 kcal/mol compared to −10.5 kcal/mol predicted by the all-electron basis set TZVP(g). SBKP was found to be a reliable basis set for $TiCl_4$, agreeing well with the all-electron result (−5.2 kcal/mol compared to −4.9 kcal/mol). It is concluded that SBKP is also a reliable basis for $TiBr_4$.

Constrained optimizations show that the dimerizations of TiF_4 and $TiCl_4$ are barrierless processes.

Acknowledgment. This work was supported by a grant from the National Science Foundation (CH-9633480). The calculations reported here were performed on IBM RS 6000 workstations generously provided by Iowa State University and on the T3E at CEWES through a DoD Grand Challenge Grant. The authors thank Dr. David Pratt for making them aware of his NMR work on $TiCl_4$. The authors also thank Dr. Jan Jensen for helpful discussions and Dr. Graham Fletcher for running parallel processor calculations on the T3E.

Supporting Information Available: Figures S1−S4 contain additional LMO plots for monomers and dimers (PDF). This material is available free of charge via the Internet at http://pubs.acs.org.

JA983339I